ELSEVIER

Journal of Non-Crystalline Solids 212 (1997) 95–116

JOURNAL OF NON-CRYSTALLINE SOLIDS

Accurate fitting of immittance spectroscopy frequency-response data using the stretched exponential model

J. Ross Macdonald *

Department of Physics and Astronomy, University of North Carolina, Chapel Hill, NC 27599-3255, USA

Received 12 July 1996; revised 2 December 1996

Abstract

A new method of accurately calculating two stretched-exponential (Kohlrausch–Williams–Watts (KWW)) models and fitting them by complex non-linear least squares (CNLS) to small-signal frequency-domain data is described and used for the detailed analysis of data for the disordered materials $Li_2O–Al_2O_3–2SiO_2$ glass at 24°C and $Na_2O \cdot 3SiO_2$ from 303 K to 398.5 K. Fitting was carried out with two different KWW models, KWW0 and KWW1, and with others, and included possible electrode polarization effects and $\epsilon_{D\infty}$, the high-frequency-limiting dielectric constant, taken as a free parameter. For conductive-system dispersion, $\epsilon_{D\infty}$ and ϵ_∞ are usually unequal. The present most-physically-appropriate KWW model, the KWW1, was much superior for the present data to all other models investigated. In particular, the power-law or 'Jonscher' model was found to be inferior for fitting the trisilicate data, contrary to earlier conclusions of Nowick and Lim, based on their comparison of the fitting utility of the power-law model and the Moynihan KWW modulus formalism. In addition, serious limitations of the modulus formalism were found and are illustrated; indicating that it should not be considered for future fitting. For the $Na_2O \cdot 3SiO_2$ data, very-high-accuracy CNLS KWW1 fitting disclosed a small change in activation energy near 341 K and somewhat irregular, but well-determined, temperature dependence of the β exponent of the KWW1 model. Although the differences between fit predictions and the trisilicate data are too small to distinguish on ordinary $M''(\omega)$ or $-\rho''(\omega)$ plots, the very small relative residuals of the fit nevertheless show appreciable serial correlation, rather than random behavior, indicating that some systematic errors still remain.

PACS: 66.90.tr; 77.22.Gm

1. Introduction

Stretched-exponential time response, also known as Kohlrausch–Williams–Watts (KWW) response [1–3], is frequently observed in amorphous polymers, glasses, and other disordered materials. It appears, for example, in mechanical, dielectric, NMR, dynamic light scattering, and spin-glass remnant magnetization experiments. References to both its widespread experimental appearance and to the large number of theoretical approaches which lead to such behavior are given in Ref. [4]. In spite of the experimental and theoretical interest of KWW behavior, serious problems with fitting frequency-domain data to the KWW response model have persisted. KWW data fitting, in either the time or frequency domain, is usually carried out to estimate model parameter values and adequacy of fit of the model. If the data

* Tel.: +1-919 962 2078; fax: +1-919 962 0480; e-mail: macd@gibbs.oit.unc.edu.

PII S0022-3093(96)00657-6

are temporal, weighted non-linear least squares fitting of the original data with the stretched-exponential retardation [5] function,

$$\phi(t) = \phi(0)\exp\left[-(t/\tau_0)^{\beta}\right], \quad 0 < \beta \leq 1, \qquad (1)$$

is straightforward [6]. The simpler alternative of fitting after logarithmic transformation introduces bias in at least one of the parameter estimates and should be avoided [7]. For dielectric response, Eq. (1) describes the decay of polarization after a polarizing field has been removed. The current is proportional to $-\mathrm{d}\phi(t)/\mathrm{d}t$ [2]. It is customary to take $\phi(0) = 1$ and consider a normalized distribution of relaxation times (DRT), $g_{\mathrm{k}}(\tau)$, with which $\phi(t)$ is associated [8–10] [1,2]. The distinction between retardation and relaxation times [5] will hereafter be ignored, in keeping with common usage.

Now some other important distinctions need to be made for frequency-domain behavior. First, one needs to distinguish between two types of dispersion: dielectric-system dispersion (DSD) and conductive-system dispersion (CSD). For a dielectric system, the dominant AC behavior arises from induced and/or permanent dipoles and/or from relatively localized charges which are unable to percolate throughout the material, and thus a separate treatment is required to describe any dc response present. When such dielectric response shows dispersion, it is an instance of DSD. For CSD, on the other hand, long-range mobile charges dominate the response at low frequencies, and the unblocked dc part of the total response is just the zero-frequency limit of the ac response. Although both DSD and CSD may appear in the same frequency range [10–14], the data analyses discussed herein were not found to require this complication. But note that even when there is no DSD in the frequency range where CSD is observed, a non-zero dielectric-system dielectric constant will still contribute to the total response. Here it will be denoted $\epsilon_{\mathrm{D}\infty}$. The subscripts 'D' and 'C' are used herein to denote dielectric- or conductive-system quantities, respectively. A list of principal acronyms and abbreviations is provided at the end of this work.

Most of the standard empirical frequency-response expressions, such as the Cole–Cole [15] and Cole–Davidson ones [16], were originally developed and applied for DSD situations. Nevertheless, in normalized form, they have often subsequently been employed for analyzing CSD data as well (e.g., [10–14,17,18]). This amounts to using a particular DRT, $g(\tau)$, associated with dielectric response, to describe a distribution of resistivity relaxation times. In 1972 and 1973, Moynihan and collaborators first discussed the effects of a distribution of 'conductivity' relaxation times [8,19] and described an approximate method of fitting frequency response data to a KWW model appropriate for CSD. Their approach involved describing CSD response in terms of a new DRT proportional to $\tau g(\tau)$ rather than to $g(\tau)$ [8,10]. Independently and later, a more general CSD approach involving thermally activated distributed behavior was described by the present author which, in its most likely form, also led to $\tau g(\tau)$ response ($n = 1$), rather than to DSD or CSD $g(\tau)$ response ($n = 0$) [10,20].

These results suggest that we need to distinguish two different types of possible CSD response using $n = 0$ and 1. First, define $x \equiv \tau/\tau_{on}$, where τ_{on} is a characteristic relaxation time of the response, as in Eq. (1). Then a general expression for normalized small-signal electrical or mechanical frequency response associated with a single dispersion process involving the dimensionless DRT $G_n(x, p_n) \equiv \tau_{on} G_n(\tau, p_n)$ may be written [10,20]

$$\frac{U_n(\Omega_n, p_n) - U_n(\infty, p_n)}{U_n(0, p_n) - U_n(\infty, p_n)} \equiv I_n(\Omega_n, p_n) = \int_0^{\infty} \frac{G_n(x, p_n)\,\mathrm{d}x}{[1 + \mathrm{i}\Omega_n x]}, \qquad (2)$$

where p_n represents the set of shape parameters involved for a particular DRT; U is a measured or model quantity of interest; $\Omega_n \equiv \omega\tau_{on}$; and ω is the angular frequency. Since the value of n in Ω_n will usually be clear from the context, we shall generally write Ω in place of Ω_n. For KWWn response, p_n is just β_n.

[1] The $\rho(\tau)$ function in Ref. [9] is equivalent to the present $G(\tau)$ DRT function.

[2] Eq. (8), which was present in the final proof of Ref. [10], was unaccountably omitted in the printed version. See erratum in J. Non-Cryst. Solids 204 (1996) 309. Also, the quantity G_{D} in eq. (A2) should be G_{CD}.

If we set $n = \mathrm{D}$, then $U_{\mathrm{D}}(\Omega) = \epsilon(\Omega)$, the complex dielectric constant, while for $n = C$, $U_{\mathrm{C}}(\Omega) = Z(\Omega)$ the impedance, or $\rho(\Omega)$ the complex resistivity. Alternatively and hereafter, we shall set $n = 0$ for both dielectric-level DSD response and impedance-level CSD response (i.e., CSD0) involving the same DRT. In addition, the choice $n = 1$ will be used to denote the second type of CSD response, CSD1, one which involves the original CSD0 DRT multiplied by τ (see Appendix A for more details). It is inappropriate to use a CSD1 response model to fit DSD behavior [20]. Note that because of the relations between the four immittance levels [10] and the form of Eq. (2), CSD should properly be described by a distribution of resistivity relaxation times (not conductivity relaxation times), and DSD by a distribution of dielectric relaxation times, actually equivalent to a distribution of conductivity relaxation times. Even when dispersion is not actually associated with a physical process involving a DRT, it may still be formally expressed in terms of one, as in Eq. (2).

2. General CSD relations

The minimum set of parameters for KWW fitting of $\epsilon(\omega)$ DSD data includes $\epsilon_{\mathrm{D}\infty}$, $\Delta\epsilon_{\mathrm{D}} \equiv \epsilon_{\mathrm{D}0} - \epsilon_{\mathrm{D}\infty}$, β_0, and $\tau_{\mathrm{o}0}$, where the latter two are those present in Eq. (1). Similarly, the minimum set of parameters for general KWW CSD fitting is $\epsilon_{\mathrm{D}\infty}$, $\rho_{\mathrm{C}\infty}$, $\Delta\rho \equiv \rho_{\mathrm{C}0} - \rho_{\mathrm{C}\infty}$, β_1 and $\tau_{\mathrm{o}1}$, where $n = 0$ and 1 subscripts have been partly omitted. Although $\epsilon_{\mathrm{D}\infty}$ is never zero, one usually finds that in CSD situations $\rho'(\infty) \equiv \rho_{\mathrm{C}\infty} \equiv \rho_\infty$ is zero or negligible. Since this is the case for the present data sets, the remaining parameters are $\epsilon_{\mathrm{D}\infty}$, $\rho_{\mathrm{C}0} \equiv \rho_0$, β_1, and $\tau_{\mathrm{o}1}$. It turns out that CSD response always involves important limiting CSD-related dielectric quantities which may be derived from the CSD fit parameters and moments of the appropriate KWW CSD distribution, $G_n(x,\ p_n) = G_{\mathrm{K}n}(x,\ \beta_n)$. Expressions for the related $n = 0$ and 1 dimensionless mth moments of a general $G_n(x)$ distribution, $\langle x^m\rangle_0$ and $\langle x^m\rangle_1$, are given in Appendix A. The limiting CSD dielectric quantities for a general DRT for $n = 0$ and 1 [10] are

$$(\epsilon_{\mathrm{C}\infty})_0 \equiv \epsilon_{\tau 0}/\langle x^{-1}\rangle_0, \tag{3}$$

$$(\epsilon_{\mathrm{C}\infty})_1 \equiv \epsilon_{\tau 1}/\langle x^{-1}\rangle_1, \tag{4}$$

$$(\epsilon_{\mathrm{C}0})_0 \equiv \epsilon_{\tau 0}\langle x\rangle_0, \tag{5}$$

and

$$(\epsilon_{\mathrm{C}0})_1 \equiv \epsilon_{\tau 1}\langle x\rangle_1, \tag{6}$$

where

$$\epsilon_{\tau n} \equiv \tau_{\mathrm{o}n}(\Delta\rho)_n/\left[\epsilon_{\mathrm{v}}\{(\rho_{\mathrm{C}0})_n\}^2\right], \tag{7}$$

ϵ_{v} is the permittivity of vacuum, and the moments implicitly involve the distribution-shape parameter(s) p_n.

Note that if $p_0 = p_1$ and $\epsilon_{\tau 0} = \epsilon_{\tau 1}$, then the use of Eq. (A.3) in Eq. (4) leads to $(\epsilon_{\mathrm{C}0})_0 = (\epsilon_{\mathrm{C}\infty})_1$. In actual CSD0 and CSD1 fits of the same data, the above equalities do not hold, however, because the $n = 0$ and $n = 1$ fitting models are always different, causing parameter estimates to differ. This is the reason why the $n = 0$ and $n = 1$ relations are separately given above and are carefully distinguished. They were not always fully distinguished in Ref. [10]. For example, from the above relations we can write

$$(\epsilon_{\mathrm{C}0})_n/(\epsilon_{\mathrm{C}\infty})_n = \langle x\rangle_n\langle x^{-1}\rangle_n, \tag{8}$$

but in [10], $(\epsilon_{\mathrm{C}0})_1/(\epsilon_{\mathrm{C}\infty})_1$ was also inappropriately set equal to $\langle x^2\rangle_0/[\langle x\rangle_0]^2$ through the use of Eq. (A.3). Such possible errors (when the values of equivalent p_0 and p_1 parameters differ) are easy to make because the moment expressions do not explicitly show the shape parameters of the distributions involved. Note that all the CSD dielectric quantities defined above involve only CSD parameters and are independent of $\epsilon_{\mathrm{D}\infty}$. For KWW fitting, one need only use the specific KWW values of the moments in Eqs. (3)–(6) to calculate these quantities. But, as discussed later, $\langle x^{-1}\rangle_0$ is infinite for traditional KWW response [9,10].

Although Eq. (A.5) relates general CSD0 and CSD1 normalized response models at the impedance or complex resistivity level, it is desirable to also express the relationship at the electrical modulus level when $\rho_{\mathrm{C}\infty} = 0$ the situation considered by Moynihan et al. [8,19]. Then, $M_1(\Omega) \equiv i\omega\epsilon_{\mathrm{v}}\rho_1(\Omega) = i\omega\epsilon_{\mathrm{v}}(\rho_{\mathrm{C}0})_1\ I_1(\Omega,\ p_1)$. It follows from Eqs. (A.5) and (4) that

$$\begin{aligned} M_1(\Omega) &= \left[\mathrm{i}\omega\epsilon_{\mathrm{v}}(\rho_{\mathrm{C}0})_1\langle x^{-1}\rangle_1/\mathrm{i}\Omega\right] \\ &\quad\times\left[1 - I_0(\Omega,\ p_1)\right] \\ &= \left[\langle x^{-1}\rangle_1/\epsilon_{\tau 1}\right]\left[1 - I_0(\Omega,\ p_1)\right] \\ &= \left[1 - I_0(\Omega,\ p_1)\right]/(\epsilon_{\mathrm{C}\infty})_1. \end{aligned} \tag{9}$$

An expression equivalent to the final result in Eq. (9) appeared in Ref. [8] but with $(\epsilon_{C\infty})$ replaced by ϵ_s, where this quantity was defined as involving all ordinary contributions to the relative permittivity of the material except those connected with long-range ionic diffusion [19]. It can thus be identified with the present $\epsilon_{D\infty}$. Such identification led Moynihan and his associates to obtain incorrect expressions for $(\epsilon_{C\infty})_1$ and $(\epsilon_{C0})_1$, ones which improperly connected CSD and DSD quantities [8,19]. These and other limiting results of these authors have been discussed and corrected in Ref. [10].

3. KWW fitting approaches

As mentioned in Ref. [10], the CSD1 Moynihan approach, exemplified by Eq. (9) with $(\epsilon_{C\infty})_1$ replaced with ϵ_s, continues to be widely applied to the present day (e.g., [21–24]), where it is often identified as the Moynihan electrical modulus formalism (MMF), and ϵ_s is itself now usually replaced by ϵ_∞, the limiting-high-frequency real part of $\epsilon(\Omega)$. Here, let MMF denote the actual fitting procedure used by practitioners of the modulus formalism, one based on Eq. (9) with ϵ_∞ rather than $(\epsilon_{C\infty})_1$, but one which does not actually fit data directly to this equation. Now when $\rho_{C\infty} = 0$, $\epsilon_\infty = (\epsilon_{C\infty})_1 + \epsilon_{D\infty}$ always unequal to $\epsilon_{D\infty}$. On the other hand, when $\rho_{C\infty} \neq 0$, $\epsilon_\infty = \epsilon_{D\infty}$ [10]. In this less likely case, it nevertheless turns out for CSD1 behavior that when $\epsilon'(\Omega)$ decreases to $(\epsilon_{C\infty})_1 + \epsilon_{D\infty}$, it may remain at this value for an extended frequency range and then only decrease from this plateau towards $\epsilon_{D\infty}$ at frequencies possibly beyond the measured range [10]. When $(\epsilon_{C\infty})_1 > \epsilon_{D\infty}$, often the case, it is easy to identify $(\epsilon_{C\infty})_1$ wrongly as $\epsilon_\infty = \epsilon_{D\infty}$. But whatever the value of $\rho_{C\infty}$, neither ϵ_∞ nor $\epsilon_{D\infty}$ should appear in Eq. (9), and $\epsilon_0 = \epsilon_{0n} = (\epsilon_{C0})_n + \epsilon_{D\infty}$.

The major problem in fitting frequency-response data to a KWW model is that an analytic expression for $G_{Kn}(x, \beta_n)$ is unavailable, except for the special choice $\beta_0 = 0.5$ [9,10], so that Eq. (2) cannot be used for the calculation of $I_{Kn}(\Omega, \beta_n)$. Although other integral expressions are available for this complex quantity [3,25,26], they involve rapidly oscillating integrands and are correspondingly difficult to use for accurate calculations and fitting involving numerical integration, particularly for $\beta_n < 0.5$.

In the work of Moynihan et al. [8], numerical approximations to $G_{K0}(x, \beta_0)$ for given β_0 values were obtained by a linear inversion approach, one which has been discussed and compared with a superior approach in Refs. [10,27]. The Moynihan analysis method [8], the MMF, is essentially a 'few-point' CSD1 fitting procedure which allows estimates of parameters such as τ_0, β, and ϵ_∞ (*not* $(\epsilon_{C\infty})_1$) to be obtained from a few values of the frequency-response data of the imaginary-part of the complex modulus. The method tends to emphasize points near the peak of the $M''(\omega)$ data curve, is *very* approximate and fails to properly distinguish $n = 0$ and $n = 1$ quantities (see later discussion), takes no account of other processes such as electrode effects which can influence the measured results [10,13,14], and even when automated [21] it is inappropriate for complex non-linear least squares (CNLS) fitting of the data. The use of the modulus formalism has been strongly criticized by Elliott [28], and some of its errors are identified and discussed in Ref. [10]; in addition, Dyre [29] has pointed out that the shape of the $M''(\omega)$ peak is not of fundamental significance. These matters are of no particular importance, however, when CNLS fitting is employed. With proportional weighing [10,13,14,27,30] [3], CNLS fitting yields exactly the same parameter estimates whether data at the modulus or complex resistivity level is analyzed (e.g., compare the model expressions given in Eqs. (A.5) and (9)), uses all data points, and readily allows one to take account of all processes thought to contribute to the measured response. But the use of CNLS fitting requires that one be able to calculate the fitting model accurately and quickly for any values of its parameters. The present work shows how this may be done for the CSD0 and CSD1 KWW response models and illustrates the utility of the CNLS approach.

Consider now fitting to a KWW frequency response model. Since CSD0 and CSD1 response models may be used to fit data at any of the four

[3] The latest version of the LEVM CNLS fitting program, V. 7.0, may be obtained at no cost from Solartron Instruments, Victoria Road, Farnborough, Hampshire, GU147PW, United Kingdom. E-mail, attention Dave Bartram, bartram@solartron.com.

immittance levels, and since the modulus level holds no favored position, the designation KWW-CSD1, or KWW1, is more appropriate than 'modulus formalism' to designate such KWW fitting models and approaches. Therefore, KWW0 and KWW1 will be used hereafter, and 'modulus formalism' will be taken to mean only the few-point Moynihan CSD1 fitting approach [8], the MMF. In Ref. [10], CSD1 models and fitting were identified by Class-A and CTM, and CSD0 models and fitting by Class-B and CSD, but the present notation is preferable. Note that n is the power of τ present in the DRT $\tau^n G_0(\tau)$.

Another few-point KWW fitting approach was proposed by Weiss, Bendler, and Dishon [26]. It was applied only for DSD situations, however, and thus used only $\epsilon''(\omega)$ data for parameter estimation. These authors made the important observation, which applies to all KWW few-point fitting approaches, that "...the physical assumption that the system is characterized by a single degree of freedom may not be valid, with the consequence that the Williams–Watts model will not be a useful tool for describing the data." While the first part of this quotation is true, the second part need not follow when CNLS fitting is employed.

In an effort to overcome the difficulty in adequately fitting frequency data to a KWW model, an approximate KWW0 fitting algorithm was developed [17] based on the accurate KWW0 response tables of Ref. [25]. It was incorporated in the LEVM CNLS fitting program [30] and has been available since 1986. It can be used to analyze either DSD or CSD data, and, since it is a part of the general LEVM program, all other processes likely to be present may also be included in the full fitting model. Although this KWW0 approximate model, denoted by AKWW hereafter, is accurate enough for fitting most noisy data, it is far less accurate when converted to KWW1 response using Eq. (A.5), particularly in the low-frequency region where $[1 - I_0'(\Omega, p_1)]$ becomes very small.

Therefore, a new approximate KWW0 model has been developed whose relative errors are so small (less than one part in a million for any β value of experimental interest), that fit errors are completely negligible for either the KWW0 or its KWW1 extension model. As described in Appendix A, the new approach uses two types of series and a convergence-enhancing procedure to achieve this accuracy, yet it allows rapid CNLS fitting. Here, the utility of the new approach will be illustrated for data involving two different disordered materials, but extensive efforts to discover more appropriate fitting models than the KWW ones will be deferred. All CNLS fits in the present work were carried out using a new version of LEVM, one which incorporates the present KWW0 and KWW1 models. It become available for free distribution in January 1997. Propor-

Table 1
Results of KWW CNLS fitting of 24°C Li_2O–Al_2O_3–$2SiO_2$ data. Here $A|B$ indicates the estimate of the quantity, A, and its estimated relative standard deviation, B. All quantities shown without such uncertainties were calculated from other fitting estimates

Column	A	B	C	D
Method/model	KWW0	KWW0-S	KWW1	KWW1-S
S_F	0.0161	0.0313	0.0129	0.0245
$10^{-9}\rho_0$ (Ω cm)	1.076|0.0033	1.075|0.0057	1.076|0.0026	1.075|0.0042
ϵ_τ	11.59|0.012	11.57|0.015	0.7355|0.0028	0.7865|0.023
$10^4\tau_0$ (s)	11.04	11.01	0.7008	0.7486
$10^3\langle\tau\rangle$ (s)	1.963	1.948	2.450	2.444
β	0.5350|0.0071	0.5368|0.0049	0.3598|0.0012	0.3637|0.0035
$10^9 B_E$	8.25|0.013	–	8.30|0.010	–
n_E	0.525|0.013	–	0.550|0.011	–
ϵ_E	74.0|0.027	–	92.0|0.016	–
ϵ_x	9.429|0.0053	9.433|0.0050	5.752|0.0075	5.653|0.0095
$\epsilon_{C\infty}$	0	0	3.370	3.478
ϵ_∞ extr., calc.	8.363, 9.429	9.433, 9.433	8.299, 9.122	9.131, 9.131
ϵ_{C0}	20.61	20.46	25.71	25.59
ϵ_0 extr., calc.	∞, 30.04	31.41, 29.89	∞, 31.46	31.24, 31.24

tional weighing was used, and Eq. (A.5) with $\langle x^{-1}\rangle_1 = \beta_1/\Gamma\{1/\beta_1\})$, rather than Eq. (9), was employed for KWW1-model fitting. Most CNLS fitting was done with the data expressed in complex resistivity form, or equivalently, modulus form, but fitting results for the other two levels were also routinely examined and were found to be quite comparable.

4. Fitting of Li_2O–Al_2O_3–$2SiO_2$ frequency-response data

Frequency-response data for the Li_2O–Al_2O_3–$2SiO_2$ glass were kindly provided by Professor Moynihan [31]. Since they have been analyzed previously by several authors and, most recently, by fitting them to the AKWW model using CNLS [10], it is worthwhile to provide accurate fit results for this data set, both to allow comparison with other published fit results and for future comparison using different fitting models.

Results of four different CSD KWW fits are presented in Table 1. The quantity S_F is here taken as the standard deviation of the relative residuals and is thus a measure of the goodness of fit. It has been alternatively defined as the standard deviation of the weighted residuals. The definitions are the same for proportional weighing. Here, proportional weighing using model values (FPWT) [30], rather than that using data values (PWT), was usually used for fitting, but the differences in results were found to be negligibly small. All parameter estimates shown without estimated relative standard deviations in Table 1 except the first value of the ϵ_∞ and ϵ_0 pairs, were calculated from Eqs. (3)–(7) using fit estimates of the parameters. The initial values shown for ϵ_∞ and ϵ_0 are fitting-model extrapolations. Subscripts distinguishing between the $n = 0$ and $n = 1$ parameter estimates are unnecessary here and are omitted below except when needed for clarity. Assume now that the dominant dispersion is of CSD1 rather than CSD0 type. The fitting parameters for the bulk dispersion are ρ_0, ϵ_τ, β, and ϵ_x, where ϵ_x is $\epsilon_{D\infty}$ for CSD1-model fitting and is approximately ϵ_∞ (see below) for CSD0 fitting. The difference arises because $(\epsilon_{C\infty})_0 = 0$ (or is very small for cutoff distributions), and thus the separate CSD0 ϵ_x free fitting parameter tries to compensate to match the data. Therefore, CSD0 fitting does not allow separate estimation of $\epsilon_{C\infty}$ and $\epsilon_{D\infty}$ for the assumed conditions. If KWW1 fitting is most appropriate for the data, the KWW0-fit ϵ_x will actually approximate $\epsilon_\infty = (\epsilon_{C\infty})_1 + \epsilon_{D\infty}$, not $(\epsilon_{C\infty})_0 + \epsilon_{D\infty}$. One can alternatively use τ_0 rather than ϵ_τ as a fitting parameter, but there are some advantages in the latter choice [10,13,14].

Some fits have been made with exact simulated data in order to clarify the conditions which lead to various ϵ estimates. In carrying out CNLS fits, as in the present work, $\epsilon_{D\infty}$ is always included as a free fitting parameter. When fitting CSD0 data with a CSD0 model, one obtains a direct fit estimate of $\epsilon_{D\infty}$ and can obtain an estimate of ϵ_∞ by evaluating the model at a very high frequency using parameter estimates from the fit. In this case, the $\epsilon_{D\infty}$ and ϵ_∞ estimates are the same since $(\epsilon_{C\infty})_0$ will always be negligible. In cases where the data are noisy and/or the model is not fully appropriate, the fit estimate of $\epsilon_{D\infty}$ may be zero. Then the extrapolated ϵ_∞ estimate will still approximate $\epsilon_{D\infty}$. When one fits CSD0 response with a CSD1 model, very poor results are obtained when $\epsilon_{D\infty}$ is taken free. When it is fixed at zero, one again obtains an approximate estimate of ϵ_∞ either from extrapolation (when fitting with Eq. (A.5)) or from $(\epsilon_{C\infty})_1$ when using Eq. (9).

In the case of most present interest, where the data involve CSD1-type dispersion, some of the results are different. When CSD1 fitting is carried out, one obtains both $\epsilon_{D\infty}$ and $(\epsilon_{C\infty})_1$ estimates when using Eq. (9), and their sum agrees with the extrapolated ϵ_∞ estimate. When $\epsilon_{D\infty}$ is taken fixed at zero, however, the free $(\epsilon_{C\infty})_1$ parameter is forced to estimate ϵ_∞, and no $\epsilon_{D\infty}$ estimate is available. When fitting involves the Eq. (A.5) form, $\epsilon_{D\infty}$ and ϵ_∞ estimates are available, and one must estimate $(\epsilon_{C\infty})_1$ from their difference. Again in this case, if the $\epsilon_{D\infty}$ fitting parameter is taken fixed at zero, or forced to this value by the fitting, an ϵ_∞ estimate may be obtained by extrapolation but no separate $\epsilon_{D\infty}$ and $(\epsilon_{C\infty})_1$ estimates are then available. Note that the results shown in Table 1 are in accord with the present conclusions. These results also show why for the MMF model, which takes no account of $\epsilon_{D\infty}$, the $(\epsilon_{C\infty})_1$ parameter of Eq. (9) must be re-interpreted as ϵ_∞, as has been done in recent times by Moynihan

[22]. However this ϵ_∞ value must not be used in Eq. (4).

In addition to the fitting parameters discussed above, the fits of columns A and C include three electrode-polarization parameters. Their effect is in series with that of the bulk response and may be expressed at the complex conductivity level as

$$\sigma_E(\omega) = i\omega\epsilon_v\epsilon_E + B_E(i\omega)^{n_E}, \qquad (10)$$

the combination of a capacitance and a constant-phase-element (CPE) in parallel [10,30]. Further discussion of such effects appears in Refs. [10,13,14]. Eq. (10) will be referred to here as the electrode response model (ERM), although other expressions are of course possible.

There are three reasons why the additional response expression of Eq. (10) has been associated with the electrodes. The first, a necessary but not sufficient condition, is that best-fit results are obtained when this contribution is in series with the rest of the response, here that associated with CSD and possible DSD processes, which are in parallel. The second is that the form of Eq. (10) has been successfully used for other disordered-material situations and electrochemical impedance spectroscopy data and is appropriate for describing space charge, diffusion in the electrode, and rough-surface electrode effects [12–14,32,33]. But no electrode-process identification is certain unless one can show that the electrode parameters obtained from fitting at the conductance or impedance level are independent of the electrode separation of the cell, requiring measurements at constant temperature for cells with two or more separations. Although such data are not available for either of the materials considered herein, recent unpublished work of the author on data for $CaTiO_3$:30%Al^{3+} of Nowick at 575 K with separations of 1.28 mm and 2.98 mm [31] strongly suggests that the ERM part of the fitted response is indeed thickness independent within experimental uncertainty.

The column-B and -D fits, designated with -S, involved subtraction from the data of the effects of the electrode polarization parameters shown in columns A and C, an easy process with LEVM, and subsequent refitting. The resulting larger values of S_F are associated with the subtraction process, one which may involve some small differences between nearly equal quantities. Comparison of the results shown in columns A and B and in C and D indicates that the elimination of estimated electrode effects changes all remaining parameter estimates slightly. The CPE is physically unrealizable in the limit of high frequencies [34] and requires a high-frequency cutoff to be made physically realizable when $n_E < 1$. In addition, it leads to $\epsilon'(\omega) \to \infty$ as $\omega \to 0$, as in columns A and C.

Note that only for the column-B and -D fits does the relation $(\epsilon_\infty)_n = (\epsilon_{C\infty})_n + \epsilon_{D\infty}$ hold exactly. These results suggest that CSD1 is preferable to CSD0 fitting, as also indicated by earlier analyses [8,10,20]. In addition, comparison with earlier AKWW CNLS fits of the present data [10] indicates fairly good agreement between the CSD0 fits, but poor agreement between the CSD1 ones. For example, estimates of β_1 near 0.47 obtained earlier [10,22] are quite different from the values in columns C and D. Thus, the present work shows that accurate KWW1 CNLS fitting is required here in order to obtain the most meaningful parameter estimates.

The LEVM fitting routine allows either ϵ_τ or τ_0 to be taken as a free parameter. As discussed elsewhere [10,13,14], one may generally expect smaller parameter cross-correlations with ϵ_τ rather than τ_0 taken free, and ϵ_τ is particularly diagnostic for comparing results at different temperatures. When fitting was carried out with τ_0 free, values very close to those shown in the table were obtained, but their relative standard deviations were appreciably larger than those listed for ϵ_τ. Although the table shows that KWW0 ϵ_τ estimates are more than 14 times larger than the KWW1 ones, reflecting a similar ratio for the τ_0 estimates, note that the $\langle\tau\rangle$ estimates show much less variation because they are averages over the full data. Finally, it is clear that the β estimates do not satisfy the relation $\beta_0 + \beta_1 = 1$. This failure does not arise because of errors in the data but because of the intrinsic differences between KWW0 and KWW1 response. To confirm this conclusion, exact KWW1 data were generated using the parameter values of column C. Fitting these data with the KWW0 model led to $S_F = 0.006$ and $\beta_0 = 0.526|0.003$. Similarly, when the same process was carried out with electrode polarization effects removed, the result was $S_F = 0.037$ and $\beta_0 =$

0.566|0.006, where this notation is defined in the caption of Table 1.

Although tabular fitting results, which are always averages, can be instructive and interesting, it is also useful to consider the point-by-point details of the shape of the data and its fits at one or more immittance levels. For the present data, this has already been done in Ref. [10] and need not be repeated here in the same format, even though the present fits are different and better than the earlier ones. An important conclusion of the earlier work was that electrode effects were not negligible both at low and at high frequencies, and that taking them into account could explain the appreciable excess high-frequency loss evident in earlier fittings of the present data (e.g., [8,22]) and termed endemic to the vitreous state by Moynihan and his associates [8]. It now appears that this effect is just an artifact arising from inadequate, few-point, modulus-formalism fitting of data, a procedure which deals only with the main dispersion process. In fact, Elliott [35] recently raised the question of whether such excess loss arose from a failure of the KWW model or from the presence of an additional dispersive contribution significant at high frequencies. Although the latter choice, electrode effects here, seems to be the dominant contributor, the situation requires a closer examination, one only practical with CNLS fitting.

Conventional plots of data and fit versus log frequency exhibit little or no visible discrepancy between the two when the fit is as good as the present ones, so greater resolution is required. This may be provided by plots of the relative residuals themselves versus log frequency. Fig. 1 shows such a plot for the real and imaginary relative residuals for the complex resistivity fit of column D of Table 1. The lines are included here to guide the eye. Since CNLS fitting with proportional weighing leads to exactly the same parameter estimates for modulus-level fitting as those obtained from fitting the data at the complex resistivity level, the residuals must also be the same. But the real and imaginary parts are reversed. Thus, $r''_\rho = r'_M$ and $r'_\rho = r''_M$, so the figure actually shows both types of residuals. The residuals directly indicate percent difference between model predictions and data values. Thus the left-most r''_ρ value, of about -0.1, corresponds to a 10% difference. Since the S_F value for column D is considerably larger than that of column C, we should expect the residuals for the latter fit to be smaller. They are not presented here because only the first few r''_ρ ones at the low-frequency end and the last few r'_ρ ones at the high-frequency end are smaller. For example, for r''_ρ the -0.1 value is reduced to -0.014, and the first positive peak value of 0.037 is reduced to 0.020. The more central residuals remain nearly unaltered.

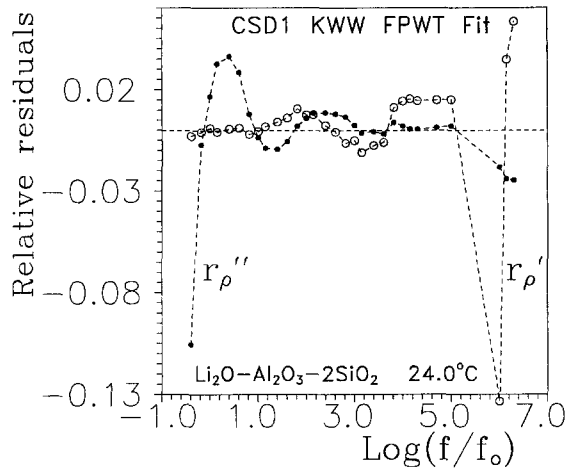

Fig. 1. Frequency dependence of real- and imaginary-part relative residuals obtained from fitting of frequency-response data of $Li_2O-Al_2O_3-2SiO_2$ glass at 24°C using the KWW1 bulk response model; see Col. D results in Table 1. Here and hereafter, $f_0 \equiv 1$ Hz, and lines between points are provided to guide the eye.

Fig. 2 shows the relative residuals obtained when the data of column D were changed by eliminating the first low-frequency point and the last three high-frequency ones. Fitting then led to $S_F \simeq 0.008$. The present results indicate that the dominant relative residuals are those of r'_M in the low-frequency region and those of r''_M at the high-frequency end. It is likely that the low-frequency ones arise from a somewhat inadequate expression for the electrode-polarization model, one whose defects are greatly amplified in the $M' \ll 1$ region when subtraction is carried out. The recognition of such a possibility is the first step towards improvement of the model. On the other hand, the last three high-frequency points of the original data are separated from the other points by a large frequency ratio and are irregular. This difference suggests that the corresponding three r''_M residuals arise primarily from systematic errors in the data, perhaps associated with the use of a different measuring instrument in this region.

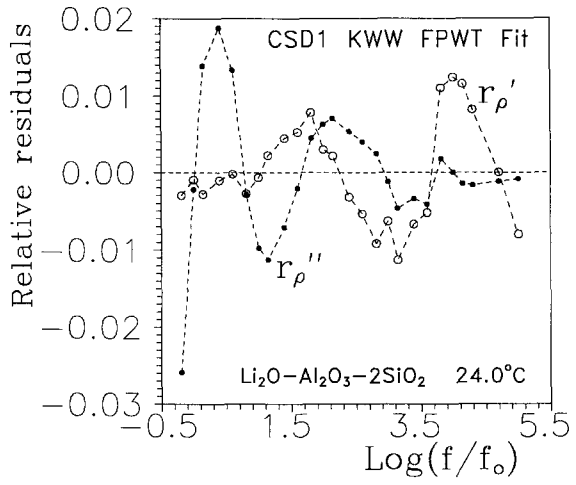

Fig. 2. Same as Fig. 1 except that the lowest frequency and the three highest frequency points were removed from the data before re-fitting.

It is important to point out that plots of $M(\omega)$ emphasize the high-frequency part of the data, as compared to $\rho(\omega)$ ones. Thus, in linear plots, differences (residuals rather than relative residuals) between M'' data and fit predictions show up better than do the ρ' ones to which they are related. Therefore, linear plots of $M(\omega)$ should be used to illustrate high-frequency discrepancies, and ones of $\rho(\omega)$ should be used for low-frequency ones. Finally, although some small random contributions are evident in the central residuals of Fig. 2, it is clear that these residuals are primarily dominated by systematic long-period, high-serial-correlation behavior, possibly indicating that even the KWW1 model is not entirely appropriate for the present data.

5. Cutoff effects

The KWW fitting results and the ϵ_C calculated values shown in Table 1 were all obtained from fits using the series approach discussed in Appendix A. Thus, they do not and cannot include any cutoffs of the generally unknown KWW $G_{K0}(x, \beta_0)$ distribution. But, as discussed elsewhere [10,34], $I_{K0}(\Omega, \beta_0)$ response is not physically realizable in the high frequency limit, where it leads to infinite conductivity. Thus, it is of interest to consider the effect of cutoff on KWW response, which can be readily done for the known $G_{K0}(x, 0.5)$ distribution, since its response models with cutoffs are included in LEVM [10]. Highly accurate numerical quadrature calculations of $I_{Kn}(\Omega,0.5)$ with cutoff were carried out in terms of the variable $y \equiv \ln(x)$, not over its full $\pm\infty$ range, but from $-\infty < y_{min} = \ln(x_{min}) < 0$ to $0 < y_{max} = \ln(x_{max}) < \infty$. For convenience, we take $|y_{min}| = y_{max} \equiv u > 1$. This choice leads to $x_{min} = \exp(-u)$ and to $x_{max} = \exp(u)$. Finally, using the relation $\omega\tau \equiv \Omega x$, we can set $\Omega_{min} x_{max} = \Omega_{max} x_{min} = 1$. Now the cutoff at $x = x_{max}$ usually has little or no effect, since for reasonable values of x_{max}, Ω_{min} will be below the natural low-frequency rolloff of KWW response, that where it approaches its limiting single-time-constant Ω behavior [10]. Thus, the major effects of cutoff should appear at the high-frequency end of the response range, that where cutoff enforces final high-frequency-limiting single-time-constant Ω^{-1} behavior of $-I''_{Kn}(\Omega)$.

For KWW0 fitting, Table 1 shows that $(\epsilon_{C\infty})_0$ is zero. With no cutoff, the moment $\langle x^{-1}\rangle_0$ is infinite, but for the present $\beta = 0.5$ KWW case, it approaches $(\pi x_{min})^{-1/2}$ as x_{min} becomes smaller and smaller [10]. For example, for $u = 5$, 10, 20, and 40, its values are about 6.68, 83.6, 1.24×10^4, and 2.74×10^8, respectively. Thus, $(\epsilon_{C\infty})_0$ is finite and non-zero when the distribution is cut off.

To show explicitly the effects of different cutoff values of u at limiting high and low frequencies, accurate data were calculated for the $\beta = 0.5$ KWW0 and KWW1 response models, both for the choice $\epsilon_\tau = 10$. As already discussed, when β_n and $\epsilon_{\tau n}$ are the same for these two models, $(\epsilon_{C\infty})_1$ and $(\epsilon_{C0})_0$ are equal. Because cutoff, particularly when it is extreme, will affect the values of the moments present in Eqs. (3)–(6), one may expect some dependence of the limiting ϵ_C values on the size of u. The values found for $(\epsilon_{C\infty})_0$, $(\epsilon_{C\infty})_1$, and $(\epsilon_{C0})_1$ were, respectively, for $u = 40$: 3.65×10^{-8}, 20, and 60; for $u = 20$: 8.05×10^{-4}, 20.0001, and 60.0001; for $u =$ 10: 0.120, 20.08, and 60.0001; and for $u = 5$: 1.5, 20.97, and 60.004. Since fitting results for wide-frequency-range real data generally show that $u > 15$, it is clear that for the $\beta = 0.5$ case at least, reasonable cutoff values will have negligible effect on all quantities but $(\epsilon_{C\infty})_0$. But since $(\epsilon_\infty)_0 = (\epsilon_{C\infty})_0 + \epsilon_{D\infty}$ and since ϵ_∞ cannot be less than unity, $(\epsilon_{C\infty})_0$ may

generally be ignored with little loss of accuracy. To express these results another way, for analyzing most experimental KWW data it seems very likely that the present no-cutoff series fitting models will be quite satisfactory.

6. Fitting of $Na_2O \cdot 3SiO_2$ frequency-response data

6.1. Fitting results for $T = 321$ K data

In evaluating and illustrating accurate CNLS KWW fitting it is important to consider data for a range of temperatures. Thanks to the kindness of Professor Nowick [31], the data on $Na_2O \cdot 3SiO_2$ which Nowick and Lim (abbreviated NL hereafter) analyzed in Ref. [11] were made available to me. The $M''(\omega)$ data curves for those temperatures to be considered herein are shown in Fig. 3. The windowing effect of a constant frequency range for different temperatures is clearly evident. Had $-\rho''(\omega)$ curves been plotted, it would be evident that at 303 K not even the peak of the curve is reached at 10 Hz. The relation between the peak frequencies of M_1'' and $-\rho_1''$ model predictions is illustrated later for the present material.

The present data were earlier analyzed by the MMF approach at the Naval Research Laboratory and results appear in Ref. [11]. Particular attention was devoted in Ref. [11] to fitting results for the 321 K data. As usual for modulus-formalism fitting, the calculated response fell below the data points in the high-frequency tail, as expected from the foregoing results and discussion. Several fits have been carried out to demonstrate the phenomenon and its cure. Their results appear in Fig. 4 and in Table 2. In an effort to duplicate some features of electric-modulus

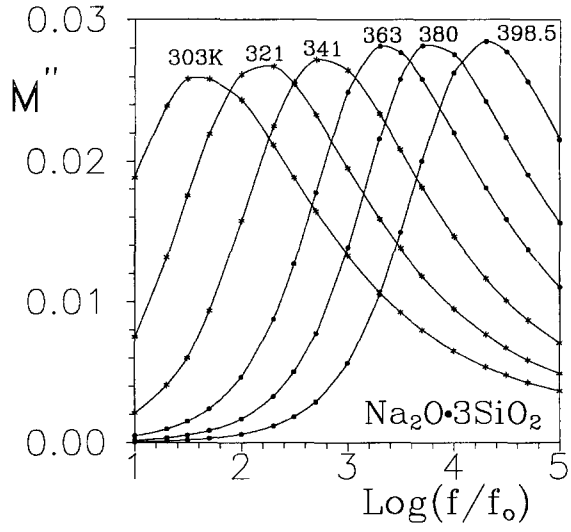

Fig. 3. Variation of measured $M''(\omega)$ data with frequency for the $Na_2O \cdot 3SiO_2$ glass at six temperatures.

behavior, CNLS KWW1 fitting with unity weighing (UWT) was first carried out. Such weighing emphasizes response around the $M''(\omega)$ peak region. First, all the model parameters were taken fixed at the values quoted by NL except ρ_0 and $\epsilon_{D\infty}$ (a quantity not considered by NL), both of which were allowed to vary. As shown in Table 2, such fitting yielded a large value for S_F, a zero estimate for $\epsilon_{D\infty}$, and a ρ_0 value appreciably different from those obtained with much more accurate fits. The corresponding fit curve in Fig. 4 shows the expected behavior. Appreciably better results were obtained when all parameters were taken free in the fitting, but some high-frequency discrepancies are still evident.

Although the fit is further improved when PWT is employed instead of UWT, it is still unsatisfactory.

Table 2
Results of CNLS fitting of 321 K $Na_2O \cdot 3SiO_2$ data to the KWW1 model for various weighing choices without (first three lines, last line) and with electrode polarization parameters

Weighing, par.	S_F	β	$10^4\tau_0$ (s)	ϵ_τ	$10^{-9}\rho_0$ (Ω cm)	$\epsilon_{D\infty}$
UWT, ρ_0 free	0.18	0.5	8.0	5.16	1.753|0.006	0
UWT, free	0.048	0.321|0.111	0.488	0.358|0.80	1.540|0.021	7.09|0.11
PWT, free	0.035	0.327|0.120	0.523	0.401|0.87	1.475|0.012	6.85|0.14
PWT, el., free	0.0025	0.425|0.069	2.42	1.90|0.38	1.441|0.010	4.80|0.19
PWT, el. fixed	0.0023	0.425|0.003	2.42	1.90|0.02	1.441|0.001	4.801|0.013
PWT, el. subtr.	0.0027	0.425|0.003	2.42	1.90|0.02	1.441|0.001	4.802|0.013

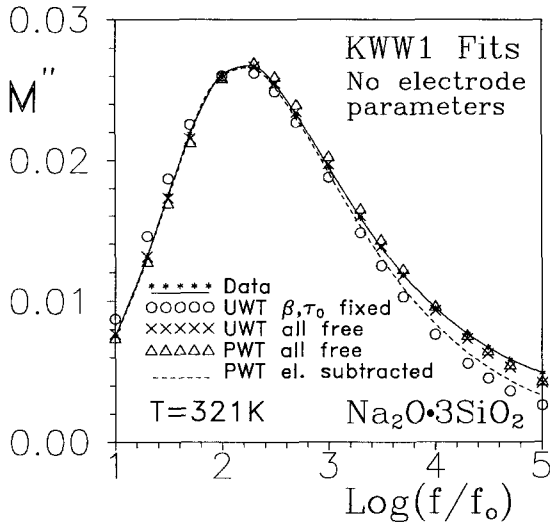

Fig. 4. Plot of original M'' data and KWW1-model fits for the sodium trisilicate glass at 321 K. See the specific parameter estimates for these fits listed in Table 2. Except for the last proportional-weighing (PWT) curve (see the last row in Table 2), no correction for electrode effects has been made in obtaining these fitting results. The unity-weighing (UWT) fit with β and τ_0 fixed uses the Nowick-Lim [11] values obtained by modulus-formalism KWW fitting at the Naval Research Laboratory (see the results shown in the row with ρ_0 free in Table 2).

As shown by the results in Table 2, S_F is decreased by a factor of more than ten when the full fitting model includes the three electrode parameters of Eq. (10). Note that the estimated relative uncertainties of most of the bulk parameters are greatly reduced when the electrode parameter values are either taken fixed at their CNLS estimated values or their effects are subtracted from the data. When electrode effects are included, the fit is so close that its predictions are indistinguishable from the data within appreciably less than the width of a line and are thus not included in Fig. 4. On the other hand, the dashed line shows the response when electrode effects are removed and the KWW1 model, without the Eq. (10) addition, is then fitted to the revised data.

The present results again show that accurate KWW1 CNLS fitting is far superior to the approximate MMF method, and that the full fit with electrode parameters included yields KWW1 parameter estimates completely in consonance with those obtained when data with electrode effects subtracted are fit with the KWW1 model. Although this latter fit is exceptionally good and involves no readily identified remaining low- or high-frequency electrode-effect residuals, the very small fit residuals nevertheless still show dominant serial correlation. Unless this is associated with systematic measurement errors, it appears that the KWW1 model is not quite ideal for fitting the present data. But for practical purposes, including parameter estimation, it is nevertheless quite satisfactory; it is the best one found so far for the present data; and the present fit is probably the most accurate KWW frequency-response one carried out to date.

Before considering KWW1-fit temperature-dependence results, it is worthwhile to present a few fitting results obtained with bulk-response models different from the KWW1 one. First, Table 3 shows that the KWW0 model leads to a somewhat smaller S_F value than the last three KWW1 results shown in Table 2. Since the KWW0 is, however, less theoretically appropriate than the KWW1 and does not allow

Table 3
Comparison of PWT CNLS fitting of 321 K Na2O · 3SiO$_2$ data with various models. The first three rows involve CSD0 fitting and the last ones involve combined CSD1 and DSD fitting. Here ψ is the ZC exponent and ϕ is associated with the exponential distribution of activation energies (EDAE) model

Type	$10^2\ S_F$	β, ψ, ϕ	$10^{-9}\ \rho_0$ (Ω cm)	$10^3\ \tau_0$ (s)	ϵ_τ	ϵ_x
KWWO-el.	0.16	0.536|0.001	1.436|0.0007	1.321	10.39|0.002	10.29|0.001
ZC-no el.	2.05	0.642|0.006	1.565|0.007	1.446	10.43|0.020	9.412|0.004
ZC-el.	1.17	0.692|0.032	1.479|0.055	1.400	10.69|0.039	10.25|0.056
KWW1/	0.20	0.406|0.018	1.460|0.0007	0.190	1.467|0.105	0
EDAE-no el.		−0.058|0.10		0.059|0.13		5.30|0.05
KWW1/	0.09	0.457|0.029	1.436|0.004	0.352	2.770|0.151	0
EDAE; el.		−0.042|0.038		0.119|0.15		3.69|0.13

separate estimation of $\epsilon_{D\infty}$, it will not be considered further. Table 2 also shows fitting results for the CSD0 ZC model [15,33,36,37], given by

$$\sigma_{ZC}(\omega) = \sigma_0\left[1 + (i\omega\tau_o)^{\psi}\right]^{\gamma},$$

$$0 < \psi \leq 1, \ \gamma = 1, \tag{11}$$

where $\sigma_0 \equiv (\rho_0)^{-1}$. A function of this form, but without the 'i', was used by Nowick and associates [11,38] for analyzing $\sigma'(\omega)$ response. It was termed the Jonscher approach, but the present full and more appropriate [36] form of Eq. (11) was introduced much earlier for CSD0 [33,39,40] and for DSD [15] analysis. When γ is variable and $0 < \gamma < 1$, Eq. (11) represents Havriliak–Negami (HN) response [41].

Nowick and Lim [11] obtained an estimate of $\psi = 0.60$ for the present data. This value is appreciably different from the ZC-fit estimates of 0.64 and 0.69 shown in Table 3. Further, the high-frequency limiting slope of $\Delta\sigma(\omega) \equiv \sigma'(\omega) - \sigma_0$ is ψ for the ZC and $1 - \beta$ for the KWW. Note, however, that this slope is the limit of the KWW1 model *alone* when an ERM is part of the full fitting model, but all fits which do not explicitly take electrode effects into account, such as that shown in the ZC-no el. line of Table 3, implicitly involve high-frequency slope estimates which include both bulk-model and ERM contributions.

On using the KWW1 fit value of β of 0.425, as in Table 2, one obtains a limiting slope estimate of 0.575, reasonably close to the 0.60 NL estimate but in disagreement with the CNLS-fit ZC ψ estimates of Table 3. In this table the first three fits are of CSD0 character and so involve the combined quantity $\epsilon_x = \epsilon_\infty$ of Table 1. Fig. 5 compares $\Delta\sigma(\omega)$ response curves for the fit of the KWW1 model to the data with electrode effects subtracted and to the data without such subtraction. It is clear that the high-frequency slope of the latter fit is appreciably greater than that of the former. By contrast, Fig. 4 of Ref. [11] shows a decreasing modulus-formalism slope at high frequencies. Further, at low frequencies the approach to the necessary limiting slope of two is evident in both of the curves of the present Fig. 5, but it is hardly apparent in the corresponding $\Delta\sigma(\omega)$ curve of NL [11], evidence for a smaller and less appropriate choice of σ_0 in that work.

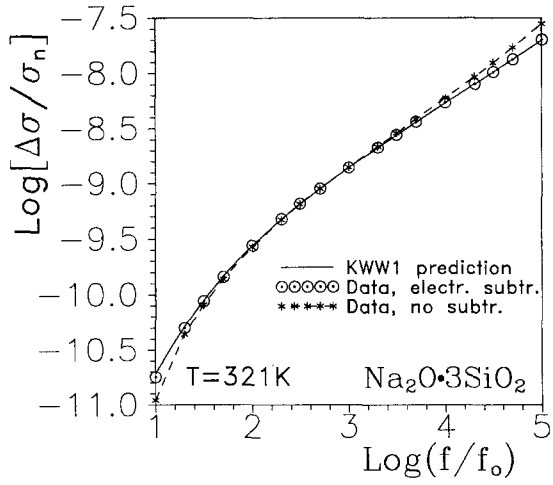

Fig. 5. Plots of $\log[\Delta\sigma(\omega)/\sigma_n]$ versus log frequency, where $\Delta\sigma(\omega) \equiv \sigma'(\omega) - \sigma_0$ and $\sigma_n \equiv 1$ s, for the original 321 K data without and with electrode effects subtracted from the data, and the predicted response for a KWW1 fit of the subtracted data (last line of Table 2).

Nowick and Lim concluded that the Jonscher fitting model they used is more meaningful than the MMF approach for the present data. They found that in order to obtain better fits with the latter at high frequencies an 'excessively high' constant-loss contribution needed to be added at all temperatures [11]. Here, by contrast, we find that electrode effects must be added in order to improve KWW1 fits at both low and high frequencies. To test the appropriateness of added constant loss, the last two fits of Table 3 were carried out. They included both a CSD1 KWW1 model and an exponential distribution of activation energies (EDAE) DSD model in parallel, as in earlier work [10,13,14]. The latter model involves a separate relaxation time, shown in the τ_0 column of the table, and an exponent-type parameter $\phi = \phi_0$, and leads to a $\Delta\sigma$ slope contribution of $1 - \phi$ for small ϕ. Only when $\phi = 0$ is one dealing with a constant-loss situation, not the case here, as shown by the EDAE results of Table 3. For these combined CSD and DSD fits, the parameter relative standard deviations are appreciable, even though the S_F values are small, in part because of the large number of highly correlated free fitting parameters involved. The ϵ_x values for the two EDAE fits are comparable to the $\epsilon_{D\infty}$

values shown for the last three KWW1 fits of Table 2. Finally, it is evident that although the ZC CSD0 model is indeed somewhat superior to the modulus-formalism one [11], the accurate KWW1 model is far superior to the ZC for the present data.

6.2. Some problems of the Moynihan modulus-formalism CSD fitting approach

Because of the widespread past usage of this formalism, it is desirable to illustrate some stumbling blocks inherent in it, ones which generally render fitting results obtained by this method inadequate. The modulus approach is so called because it primarily deals with the $M''(\omega)$ data. Consider now the task of obtaining plausible CSD1 parameter estimates by the conventional MMF approach. The usual parameters that are obtained from the data by inspection and graphical extrapolation, interpolation and fitting are ρ_0, τ_{Mdp}, β, and ϵ_∞. The τ_{Mdp} quantity is defined by $\omega_{Mdp}\tau_{Mdp} = 1$ where ω_{Mdp} is the value of ω at the peak of the $M''(\omega)$ data curve. In addition, define ω_{Mp} as the value of ω at the peak of the $M_1''(\omega)$ model response associated with Eq. (9), and τ_{Mp} as the τ associated with it. Although τ_{Mdp} and τ_{Mp} are always different for CSD situations, as we shall see, this is often unremarked or unrecognized in MMF fitting. Note that the situation is different for DSD KWW fitting since there the key frequency is that of the peak of $\epsilon_D''(\omega)$ [9] and electrode and σ_{C0} effects are usually zero or negligible.

If we now incorrectly replace $(\epsilon_{C0})_0$ by $(M'(\infty))^{-1} \equiv (M_\infty)^{-1} = \epsilon_\infty$ in Eq. (5), we obtain the modern form of a basic equation of the MMF approach:

$$\langle\tau\rangle_0 \equiv \tau_{o0}\langle x\rangle_0 = \epsilon_v \epsilon_\infty \rho_0 \sigma_o, \qquad (12)$$

when $\rho_{C\infty} = 0$ [22,42]. But this is a KWW0, not a KWW1 result, as confirmed by the use in KWW MMF analysis of $(\tau_0/\beta)\Gamma(1/\beta) = (\tau_{o0}/\beta_0)\Gamma(1/\beta_0)$ for $\langle\tau\rangle_0$, an appropriate expression for this quantity [9]. When ρ_0 and ρ_1 values are taken equal, however, one can use the Eq. (A.3) result to replace $\langle x\rangle_0$ by $(\langle x^{-1}\rangle_1)^{-1}$. Then on setting τ_{o0} to τ_{o1}, Eq. (12) becomes the same as Eq. (4) except for the difference between ϵ_∞ and $(\epsilon_{C\infty})_1$. Thus, while one may sometimes need to interpret the $(\epsilon_{C\infty})_1$ parameter in Eq. (9) as ϵ_∞ for fitting purposes, as already discussed, this substitution is improper in Eq. (4).

Inadequate distinction between CSD0 and CSD1 situations in MMF analyses also leads to problems with obtaining a meaningful estimate of τ_{o1}. Eq. (9), even with $(\epsilon_{C\infty})_1$ replaced by ϵ_∞ or $\epsilon_{D\infty}$, is a CSD1 fitting model and thus should lead to an estimate of τ_{o1}, not to the inconsistent τ_{o0} of Eq. (12). In practice, MMF analysis first obtains an estimate of τ_{Mdp} from $M''(\omega)$ data. Then this estimate is taken equal not to the KWW1-model $\tau_{Mp} \equiv (\tau_{Mp})_1$, but to $(\tau_{Mp})_0$ associated with KWW0 response. To see that this is the case, define $Q_n(\beta_n) \equiv \log[\tau_{on}/(\tau_{Mp})_n]$, a function which may be used to obtain an estimate of τ_{on} when values of $Q_n(\beta_n)$, and $(\tau_{Mp})_n$ are available. Moynihan et al. [8] provide a table of $Q_0(\beta_0)$ and Lindsey and Patterson [9] present a corrected set of its values. But although the latter authors properly relate these results to dielectric response, the former use them for MMF analysis instead of using the function $Q_1(\beta_1)$, and $Q_1(\beta_1) \neq Q_0(\beta_0)$, even for $\beta_0 = \beta_1 = \beta \neq 1$.

For example, for $\beta = 0.5$, 0.45, and 0.40, the values of $\{Q_0(\beta), Q_1(\beta)\}$ are $\{-0.1294, -0.1325\}$, $\{-0.1810, -0.1454\}$ and $\{-0.1784, -0.1581\}$, respectively. The Q_0 values are taken from [9], and it appears that -0.1810 is a misprint and should possibly be -0.1510. Values of Q_1 may be readily obtained to five significant figures or more since one can use LEVM to calculate M_1'' accurately for KWW1 response, with the ω points as closely spaced as desired. As a check of the present results, KWW1-model $M_1''(\omega)$ values were also calculated for $\beta = 0.5$ using the known KWW0 DRT expression [9,10] for this value of β. The relative accuracy of the integration was set to 10^{-9}, and the values of $\exp(Q_1(0.5))$ differed only in the sixth place for the two independent methods of calculation.

Even when one ignores the above difficulty, there is still a further problem. MMF analysis implicitly assumes that the estimate of τ_{Mdp} obtained from the data is an adequate approximation to τ_{Mp}. But this is only likely to be true when electrode effects and $\epsilon_{D\infty}$ do not appreciably perturb the peak frequency of the M_1'' curve. Since such perturbation is usually present, MMF estimation of τ_0 through the use of τ_{Mdp} is always suspect. Since it is only by CNLS fitting of the KWW1 model, as in the present work, that one

can adequately take these effects into account, it is unnecessary and not worthwhile to use the flawed MMF analysis approach.

Consider now the MMF fitting results for the present $T = 321$ K data listed in [11] and summarized in the first row of Table 2 (except for the value of ρ_0 which was not explicitly given by NL). We first note that the quoted NL τ_0 value (designated by NL as τ^*) is actually an approximation of τ_{Mdp}, one obtained by using the frequency of the peak point of the $M''(\omega)$ data, *not* the $M_1''(\omega)$ curve of the fitted KWW model. Thus we designate the NL 'τ_0' as $\tau_{M\,NL}$. We see that the $Q_1(\beta)$ value has been implicitly taken as unity by NL and no distinction made between $M''(\omega)$ and $M_1''(\omega)$. It is therefore hardly surprising that the β estimate of 0.50 differs appreciably from the present KWW1 fit estimate of 0.425.

Although the Q transformation may be carried out, there is little that can be done about the remaining problems of the MMF approach. These problems are primarily associated with the effect on the data of an ubiquitous non-zero value of $\epsilon_{D\infty}$. Its presence ensures that actual measured $M(\omega)$ data always differ from the Eq. (9) $M_1(\omega)$ KWW1 model results, even if the data were perfectly described by the model when $\epsilon_{D\infty}$ was zero. But the modulus formalism allows no explicit correction for the difference to be made since the information to do so is usually missing. Also significant, but often less important, is the effect of an ERM contribution. The most appropriate fit estimate of $\epsilon_{D\infty}$ is given in the last row of Table 2. Not shown there is the estimate of $(\epsilon_{C\infty})_1$, 5.368, leading to an ϵ_∞ value of 10.170. Thus, the use of 10.170 rather than 5.368 for the $(\epsilon_{C\infty})_1$ of Eqs. (4) and (9) will itself lead to error.

Further crucial problems arising from a non-zero $\epsilon_{D\infty}$ are well illustrated by accurate calculations of the τ corresponding to the peak of $M''(\omega)$ data with and without various contributions to the data; call this τ_{Mxp}. Because the present fit of the total data, one which includes ERM and $\epsilon_{D\infty}$ contributions and the KWW1 model, is so good, as shown in Table 2, we may use the total fit model to generate synthetic data with as many points as desired, which can then be used to obtain τ_{Mxp} estimates of very high accuracy. For the full model including $\epsilon_{D\infty}$, I find, on using the parameter estimates shown in the fourth and fifth rows of Table 2 to generate accurate data, that $\tau_{Mdp} \simeq \tau_{Mxp} \simeq 1.0142 \times 10^{-3}$ s. When the data are generated without ERM contributions, $\tau_{Mxp} \simeq 1.0271 \times 10^{-3}$ s, a minor change. Similarly when the ERM effects are subtracted from the original data and the result refitted without the ERM, as in the last row of Table 2, $\tau_{Mxp} \simeq 1.0148 \times 10^{-3}$ s, a completely negligible change. But when the data are generated without the presence of $\epsilon_{D\infty}$, one obtains $\tau_{Mxp} \simeq 3.3653 \times 10^{-4}$ s, and when the ERM effects are not included in the model as well, one finds $\tau_{Mxp} \simeq 3.4312 \times 10^{-4}$ s. It is only this last result, equal to τ_{Mp}, which is obtained from the Eq. (9) KWW1 response alone, that should be used to estimate the τ_{01} value appropriate for the model. It is thus evident that in the present situation the MMF will yield a τ_0 estimate too large by a factor of about three, even when a correct value of $Q_1(\beta)$ is used.

Moynihan has recently [42] applied the MMF to the Li_2O–Al_2O_3–$2SiO_2$ data of Section 4 using the HN fitting model, Eq. (11) with ψ and γ variable. Although he obtained an apparently good fit of the $M''(\omega)$ data except at the highest frequencies, he found that his parameter estimates led to a continual decrease of the predicted $\sigma'(\omega)$ at low frequencies, with no approach to σ_0, contrary to the behavior of the data or of a MMF KWW fit. For these reasons, he characterized the HN relaxation function as pathological, unsuited for CSD1 fitting, and he rejected it in favor of the KWW model. It is therefore worthwhile to compare proper HN CSD1 fitting predictions, using Eq. (9), with his results and with the present KWW1 ones of Table 1.

To do so, I set the I_0 function of Eq. (9) equal to the inverse of the $\sigma_{HN}(\omega)/\sigma_0$ expression of Eq. (11), obtaining I_{HN}. Now there is indeed a 'pathology' in the resulting M_{HN1} expression, one arising because for the HN model I''_{HN0} becomes proportional to ω^ψ at sufficiently low frequencies, and thus when $\psi < 1$ the quantity I''_{HN0}/ω does not approach a constant as it should [34]. Although this pathology can be eliminated by introducing a low-frequency cutoff, one possible choice in LEVM, this problem usually appears at frequencies below those commonly employed in the present area. When this is the case, one need not reject the HN model out of hand as Moynihan has done.

First, a LEVM UWT fit of the full $M''(\omega)$ data was carried out using Eq. (9), with all parameters

but($\epsilon_{C\infty}$)$_1$ fixed at the values found by Moynihan [42]. The resulting ($\epsilon_{C\infty}$)$_1$ estimate was only 1.5% larger than the value of $\epsilon_\infty (= 1/M_\infty)$ found by Moynihan, thus confirming his value and indicating that such analysis does not yield separate estimates of ($\epsilon_{C\infty}$) and $\epsilon_{D\infty}$, but only their combination. The S_F value for the fit was 0.14. Now it is a legitimate question to ask whether this is the best CSD1 HN fit possible, especially since 0.14 is a relatively large value. The next step, therefore, was to take all four parameters free to vary. The parameter estimates found were not very different from those of Moynihan with UWT but they changed appreciably with PWT and yielded a value of S_F of 0.046. The estimate of ψ was 0.97, rather than the 0.90 value of Moynihan; that of γ was appreciably smaller; and that of $\tau_0 = \tau_{HN}$ was appreciably larger. Incidentally, when $\epsilon_{D\infty}$ was also allowed to be a free fitting parameter, its estimate approached zero for all of the present fits, again indicating that it cannot be resolved for the present data from ($\epsilon_{C\infty}$)$_1$ in an Eq. (9) fit, so that it is ϵ_∞ which is actually estimated.

Next, when ERM parameters were added to the fitting model, the S_F for UWT fitting fell to 0.089 and that for PWT to 0.022. Particularly significant was that the two ψ values increased to 0.98 and 0.998, respectively. Further, neither of these fits showed the pathological behavior at the σ level discussed above, thus indicating that the introduction of electrode-polarization effects in the model and the approach of ψ toward unity allowed the HN to show non-pathological behavior in the measurement range. Finally, when CNLS fitting was carried out using the full $M(\omega)$ data, and the CSD1 HN, and ERM parameters, it was found that for the more appropriate PWT fitting the estimate of ψ iterated to unity, changing the HN to Cole–Davidson response [16], one which does not involve low-frequency HN-type pathology. The value of S_F for this fit was 0.036, and the estimates of ($\epsilon_{C\infty}$)$_1$ (here ϵ_∞), ψ, γ, and τ_{HN} were 9.80|0.01, 1.0, 0.202|0.02, and 3.97×10^{-3}|0.02 s, respectively. For comparison, the Moynihan values are 8.48, 0.90, 0.33, and 2.10×10^{-3} s. Comparison with the KWW1-fit results of column C of Table 1 and with earlier CSD0 Cole–Davidson fit results [10], shows that although the CD model is viable, the KWW1 one is the most appropriate one found thus far for these data.

It seems likely that in the past it was felt that because the modulus formalism involved $\epsilon_{D\infty}$ or even ϵ_∞, the effect of $\epsilon_{D\infty}$ was properly accounted for. As shown here, since it is actually ($\epsilon_{C\infty}$)$_1$ which is involved in Eqs. (4) and (9), it is desirable to treat $\epsilon_{D\infty}$ separately, as in all present KWW1 CNLS fitting.

In summary, the major problems of the CSD1 MMF approach are:

(a) The quantity ϵ_∞ is improperly used in place of ($\epsilon_{C\infty}$)$_1$, and τ_{01} is estimated inaccurately.

(b) The MMF does not treat the dielectric-system contribution to ϵ_∞, $\epsilon_{D\infty}$, separately. Thus, its effects in the data are not properly distinguished in the fitting model.

(c) MMF treatments take no account of electrode-polarization effects possibly present in the data.

(d) MMF fitting usually deals only with $M''(\omega)$ data; no complex non-linear least squares fits of the full complex quantities $M(\omega)$, $\rho(\omega)$, or $\sigma(\omega)$ are carried out. Weighted CNLS fitting is always preferable to NLS fitting or to graphical analysis [10,14].

Therefore, not only should the MMF not be used

Table 4
Results of PWT CNLS fitting of $Na_2O \cdot 3SiO_2$ data, with electrode effects subtracted from the data, using the KWW1 fitting model for six temperatures

T (K)	$10^2 S_F$	β	ρ_0 (Ω cm)	τ_0 (s)	ϵ_τ	$\epsilon_{D\infty}$
303	0.29	0.390|0.003	5.509×10^9|0.002	6.37×10^{-4}	1.306|0.021	5.33|0.011
321	0.27	0.425|0.003	1.441×10^9|0.001	2.42×10^{-4}	1.897|0.020	4.80|0.013
341	0.63	0.365|0.001	3.710×10^8|0.002	2.33×10^{-5}	0.709|0.007	6.85|0.003
363	0.55	0.383|0.003	8.624×10^7|0.001	6.70×10^{-6}	0.877|0.016	6.90|0.005
380	0.94	0.357|0.001	3.017×10^7|0.002	1.49×10^{-6}	0.556|0.006	7.14|0.005
398.5	1.06	0.326|0.001	1.054×10^7|0.002	2.55×10^{-7}	0.273|0.006	8.07|0.006

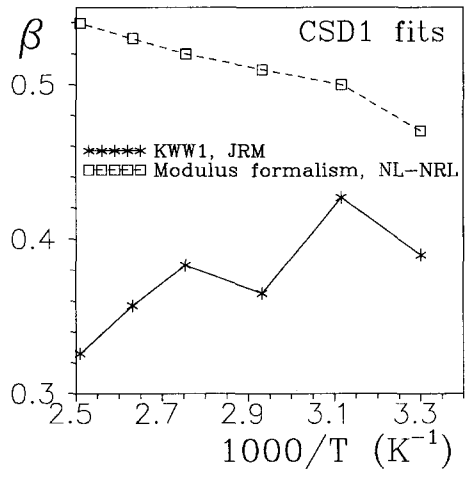

Fig. 6. Comparison of the temperature dependence of β as obtained from the present study and from the modulus-formalism analysis carried out at the Naval Research Laboratory [11].

for future KWW fitting, but all previously published results obtained with it are suspect.

6.3. KWW1 fitting results for six temperatures

Table 4 shows the KWW1-fit parameter estimates obtained for the temperature range from 303 K to 398.5 K. As noted, ERM effects were subtracted from the data using parameters obtained from CNLS fits of the original data, and then fitting was carried out without such effects. Because of the high resolution of the present fitting procedure and the evident appropriateness of the KWW1 model, some new and surprising effects are apparent in these fittings. First, Fig. 6 compares the NL β estimates with those obtained here. We have already seen that the NL MMF estimates are inappropriate; here we see unexpected behavior for the present estimates. In particular, although Table 4 shows that the present KWW1 values of β are very well determined by the data, they nevertheless show somewhat irregular temperature dependence but dependence roughly opposite to the NL-NRL MMF dependence.

Now Nowick and Lim found that their power-law exponent, identified as a slope, was 0.60, independent of temperature [11]. Although the results of ZC fitting with ERM effects included are shown in Table 3, the parameter uncertainties are mostly much greater than those obtained without taking account of such ERM contributions. Since this is opposite behavior to that found for the present KWW1 fits with and without ERM contributions, it seems likely that the difference arises because of the much greater appropriateness of the KWW1 model than that of the ZC for the present data. It is therefore likely that the 0.64 estimate obtained without ERM contributions is superior to the other ZC one listed. But, since none of the ZC-fit results takes adequate account of ERM effects, neither the NL value of 0.60 nor the 0.64 value is trustworthy. For comparison with β, the corresponding $1-\psi$ values are 0.4 and 0.36, and the mean of the present six β estimates is about 0.374.

Although there is a small possibility that the present irregular KWW1 β behavior arises from the use of an inadequate electrode polarization fitting model, and that we see in Fig. 6 just random variations about a temperature-independent mean value, the excellence of the overall fits and the fact that the ERM parameters were quite well determined over the full temperature range both suggest that, at the least, a definite temperature trend is present. Incidentally, the irregularity of the β estimates is associated with an even greater variability in the ϵ_τ estimates. Although no appropriate theory is available for CSD1 $\beta(T)$ dependence, we expect that, in agreement with the KWW1 results shown in Fig. 6, β should decrease with increasing temperature in the higher temperature range, and, in the absence of melting, approach zero, consistent with limiting Debye behavior at high temperatures where $\sigma'(\omega)$ is proportional to ω. Although the behavior of $\beta(T)$ is complicated by the possible presence of a phase change near $T = 341$ K as suggested below, it seems reasonable to expect that it should approach a constant of ≤ 1 at low temperatures; thus the reason for its final decrease at 303 K remains mysterious.

Fig. 7 shows Arrhenius plots for a variety of τ-related KWW1 quantities. Except for the $\langle\tau\rangle = \langle\tau\rangle_1$ results, the lines just connect points directly. But for the KWW1 $\langle\tau\rangle$ response, two NLS-fit sets of points are shown, covering the ranges from 303 K to 341 K and from 341 K to 398.5 K. It turns out, particularly for ρ_0 and $\langle\tau\rangle$, that the data show a definite abrupt change in slope at 341 K, as illus-

trated more specifically in Table 5. See also the change in *sign* of the slope of the β curve of Fig. 6 at this temperature. In addition to these surprising effects, which may indicate some kind of a small phase change near this temperature, Fig. 7 shows that $\langle\tau\rangle$ is exceptionally well approximated for the present data by $\tau_{\rho p}$, the τ corresponding to the peak of the $-I_1''(\omega)$ or $-\rho_1''(\omega)$ KWW1-model response curve, where $\omega = \omega_{\rho p} \equiv \tau_{\rho p}^{-1}$. Here $\langle\tau\rangle$ values are calculated as part of the LEVM fit procedure and $\omega_{\rho p}$ values were obtained by accurate, high-resolution estimation from the fitting model, as discussed in Section 6.2. To the degree that the above relation holds in general, it provides, as is evident from Eq. (6), a direct estimate of $\epsilon_v(\epsilon_{C0})_1\,\rho_0/\tau_{o1}$ without the need of anything like the $Q_1(\beta)$ function or of separate knowledge of $\langle\tau\rangle$. A preliminary check of its generality for another fit model showed that the peak approximation to $\langle\tau\rangle$ was about 9% too high at $\phi = \phi_0 = 0.4$, dropping to about 5% at $\phi_0 = 0.6$, and to about 2% at $\phi_0 = 0$ for an EDAE CSD0 fit. Note that for the EDAE response model the only difference between CSD0 and CSD1 fits arises from a difference in the ϕ_n fit value, with $\phi_0 = 1 + \phi_1$ [20].

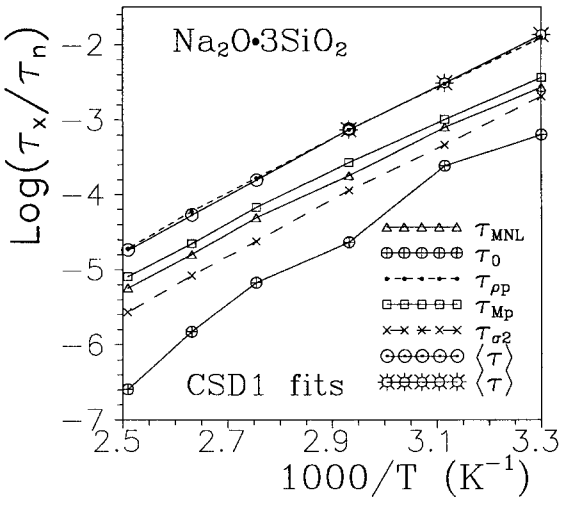

Fig. 7. Arrhenius plots for a variety of CSD1 relaxation-time estimates. Here $\tau_n \equiv 1$s. Only the two $\langle\tau\rangle$ sets of points include nonlinear least squares fit lines, for separate low- and high-temperature regions, of the original KWW1-fit results. Other lines just connect points to guide the eye. Here the subscripts 'M' and 'MP' indicate that τ was obtained from the peak of a $M''(\omega)$ or $M_1''(\omega)$ curve, and 'ρp' indicates that a $-\rho_1''(\omega)$ peak was involved. Further, the subscript '1' designates a KWW1-fit model quantity, as opposed to experimental data. $\tau_{\sigma 2}$ is the τ corresponding to the frequency at which $\sigma_1'(\omega) = 2\sigma_0$. Accurate methods of calculating some of the present quantities are discussed in the text, and the activation energies associated with the present responses are presented in Table 5.

Table 5
Activation energy estimates in eV for various quantities obtained from PWT NLS fitting of $Na_2O \cdot 3SiO_2$ fit data

Quantity	Full	Low temp.	High temp.
ρ_0: T^0	0.682|0.017	0.632|0.006	0.725|0.008
ρ_0: T^1	0.712|0.017	0.660|0.007	0.757|0.008
$\langle\tau\rangle$	0.721|0.013	0.679|0.003	0.756|0.007
$\tau_{\sigma 2}$	0.721|0.014	0.679|0.012	0.760|0.009
$\tau_{\rho p}$	0.704|0.016	0.657|0.005	0.745|0.011
τ_{Mp}	0.667|0.022	0.609|0.014	0.719|0.019
τ_{MNL}	0.673|0.021	0.634|0.058	0.706|0.031
ϵ_{C0}	0.038|0.081	0.047|0.130	0.031|0.166

Fig. 7 also shows that even though the temperature dependence of $\langle\tau\rangle$ is very regular, that of τ_o reflects the variability of β shown in Fig. 6. Thus, $\langle\tau\rangle$ is the more significant quantity here. Finally, Fig. 7 also presents accurate results for τ_{Mp}, $\tau_{MNL} \simeq \tau_{Mdp}$, and $\tau_{\sigma 2}$, where the τ_{MNL} points are those of NL, and $\tau_{\sigma 2}$ corresponds to the frequency at which $\sigma_1'(\omega) = 2\sigma_0$, the point at which the ac part of the response is generally taken to begin to become significant. The difference between the curve for τ_{Mp} and that of τ_{MNL} arises primarily, as already discussed in Section 6.2, from the presence of the effects of a non-zero $\epsilon_{D\infty}$ in the NL data, and its separate treatment in the CNLS fit, so that the KWW1-model shape and parameter estimates are unaffected by it.

Finally, Table 5 presents proportional-weighing NLS Arrhenius fits of several of the quantities discussed above. Because of the slope change most evident for ρ_0 and $\langle\tau\rangle$, fit results are shown for each quantity for the full six points and also for the three low-temperature ones and the four high-temperature ones defined above. The much smaller S_F's for most of the separate low- and high-frequency fits compared to the full fits is an indication of the reality of the change in activation energy near $T =$

341K. For completeness, activation energies are shown for fitting of ρ_0 without and with a pre-exponential factor of T. For comparison, NL found an activation energy of ρ_0 of 0.74 eV with the T factor included, a value of 0.76 eV for their ZC τ_o results, and 0.65 eV for their $\tau_{M\,\mathrm{NL}}$ (identified by them as τ_o quantities). The present results are more accurate and thus allow more discrimination. Note that if ρ_0 (with T^0) and τ_o had exactly the same activation energy, one would expect ϵ_τ to be temperature independent, not the case here [14]. It is unclear why the NL value for the activation energy of $\tau_{M\,\mathrm{NL}}$ differs somewhat from the present full-fit estimate of about 0.67.

Although the activation energy estimates for $\langle\tau\rangle$ and $\tau_{\rho\mathrm{p}}$ are close, those for $\langle\tau\rangle$ and $\tau_{\sigma 2}$ are virtually identical. Also shown in Table 5 are results for ϵ_{C0}, actually $(\epsilon_{\mathrm{C0}})_1$ here. It is evident that, in accordance with Eq. (6), the ϵ_{C0} activation energy is just the difference between that for $\langle\tau\rangle$ and that for ρ_0 (with no T factor!). It is worth remarking that the B_{E} parameter of Eq. (10) is also thermally activated. Although its dependence shows appreciable variability, it involves an activation energy of approximately 0.66 eV, suggesting that the charge carriers that are involved in the electrode response are likely to be the same as those leading to ρ_0. Finally, the $\epsilon_{\mathrm{D}\infty}$ estimates of Table 4 are approximately proportional to T, particularly for 341 K and above. This dependence may provide an initial clue concerning what proportion of the estimated $\epsilon_{\mathrm{D}\infty}$ value arises from dipole effects and how much possibly comes from localized, non-percolating charge motion [14].

7. Summary and conclusions

A new accurate method of calculating KWW frequency response has been developed and incorporated in a complex non-linear least squares fitting program. Two fitting models, KWW0 and KWW1, which involve this method, have been used to fit data for two different disordered materials. The KWW0 model is appropriate for dielectric-system dispersion and possibly for conductive-system dispersion as well, but the KWW1 model is most appropriate for CSD situations.

Outstandingly good fits of the $Na_2O \cdot 3SiO_2$ data over an appreciable range of temperatures were obtained when the total fitting model included the KWW1 model, electrode-polarization effects, and the high-frequency-limiting dielectric parameter $\epsilon_{\mathrm{D}\infty}$. Temperature dependence of many quantities, such as ρ_0 and the average relaxation time, $\langle\tau\rangle_1$, were found to involve a small but significant change of activation energy in the neighborhood of 341 K, one not evident in earlier work involving fits with lesser accuracy and resolution. The present high resolution also led to the appearance of surprising non-monotonic temperature variation in the behavior of the estimated KWW1 β exponent.

Previous analyses of these [11] and other data sets using the MMF are defective because the MMF form of CSD1 response does not allow $\epsilon_{\mathrm{D}\infty}$ to be separately estimated or estimates of the CSD1-model parameter $(\epsilon_{\mathrm{C}\infty})_1$ to be obtained. In addition, the usual modulus formalism takes no account of electrode-polarization effects. A surprising result of the present fits is that the relaxation time derived from the frequency of the peak of a $-\rho_1''(\omega)$ KWW1-model response curve (*not* that of the full data) approximates the KWW1 value of $\langle\tau\rangle_1$ closely over the full range of temperatures analyzed.

The excellence of the full CSD1 KWW fits of the $Na_2O \cdot 3SiO_2$ data makes it reasonable for the first time to suggest that future data for this material be used to try to identify the dominant source of the residual misfits. Even though the present relative residuals are extremely small, they still show long-period serial correlation. Such systematic behavior could arise from measurement errors, model inadequacy, or both. To discriminate between them, it is desirable that data over a range of temperatures have all or most of the following characteristics. First, they should extend over six to eight decades of frequency or more, with at least 10 points per decade. Measurements on the same material should be repeated using three different apparatuses: e.g., a bridge, a frequency response analyzer, and an impedance analyzer, all with replication if practical. In addition, in order to verify that the apparent electrode-process parameters needed for the full fit are not associated with extensive bulk effects, one should make measurements at the same temperature on the same material with two or more different electrode separations. Finally, unless all activation

energies turned out to be quite small, temperature control to within ± 0.1 K or better should be ensured. Some of these extreme measures would be unnecessary in future once one could either identify a measuring procedure with negligible (or random only) errors or could quantify its systematic errors so that they could be used to correct data before fitting and analysis.

8. Principal acronyms and subscripts

AKWW	An approximate KWW0 CNLS fitting model available in LEVM
C	Subscript denoting conductive
CNLS	Complex non-linear least squares
CPE	Constant-phase distributed circuit element
CSD	Conductive-system dispersion
CSD0	A type of CSD response model involving the same DRT as DSD response
CSD1	A CSD response model involving a physically reasonable modification of a CSD0 model
D	Subscript denoting dielectric
DRT	Distribution of relaxation times
DSD	Dielectric-system dispersion
EDAE	Exponential distribution of activation energies
el.	Electrode-model parameters and/or effects
ERM	Electrode response model
FPWT	Function-proportional weighing in least squares fitting; uses model values for weighing
HN	Havriliak–Negami response
KWW	Kohlrausch–Williams–Watts stretched-exponential model or response
KWW0	The present KWW response model of CSD0 type
KWW1	The present KWW response model of CSD1 type
LEVM	The CNLS fitting program used herein
MMF	Moynihan modulus-formalism CSD1 KWW fitting method
NL	Nowick and Lim, Ref. [11]
NLS	Non-linear least squares
NRL	Naval Research Laboratory
PWT	Proportional weighing in least squares fitting; uses data values for weighing
S_F	Standard deviation of the relative residuals of a NLS or CNLS fit
UWT	Unity weighing in least squares fitting; equivalent to no weighing
ZC	Cole–Cole complex DSD response model used for CSD response

Appendix A

The normalized frequency-response function, $I_n(\Omega, p_n)$, satisfies $I_n(0, p_n) = 1$ and $I_n(\infty, p_n) = 0$ in agreement with the left-hand part of Eq. (2) and requiring that the $G_n(x)$ distributions be normalized. Now the dimensionless moments of the above distributions may be expressed by

$$\langle x^m \rangle_n \equiv \int_0^\infty x^m G_n(x, p_n)\, \mathrm{d}x, \tag{A.1}$$

where the $\langle x^m \rangle_n$ clearly depend on both the shape of the distribution and on the value(s) of its p_n parameter(s). Since $\langle x^0 \rangle_0 = \langle x^0 \rangle_1 = 1$, it is necessary that

$$G_1(x, p) \equiv [x/\langle x \rangle_0] G_0(x, p), \tag{A.2}$$

where $p_1 = p_0 = p$ has been used. It then follows that [10]

$$\langle x^m \rangle_1 = \langle x^{m+1} \rangle_0 / \langle x \rangle_0, \tag{A.3}$$

so $\langle x^{-1} \rangle_1 = 1/\langle x \rangle_0$. It is worth reiterating that actual fits of data with the CSD0 and CSD1 approaches will lead to different estimated parameter values, so fit estimates of p_0 and p_1 will always be unequal.

Now let us obtain a connection between $I_0(\Omega)$ and $I_1(\Omega)$ when they both derive from a general $G_0(x,p)$ distribution. On using Eq. (A.2), we may write

$$I_1(\Omega, p_1) = \int_0^\infty \frac{G_1(x, p_1)\, \mathrm{d}x}{[1 + \mathrm{i}\Omega x]} = [\mathrm{i}\Omega \langle x \rangle_0]^{-1} \int_0^\infty \frac{\mathrm{i}\Omega x G_0(x, p_1)\, \mathrm{d}x}{[1 + \mathrm{i}\Omega x]}, \tag{A.4}$$

where $[\langle x\rangle_0]^{-1}$ involves p_1 and so may be replaced by $\langle x^{-1}\rangle_1$. The right-hand side of Eq. (A.4) may now be expressed as [10]

$$I_1(\Omega, p_1) = [\langle x^{-1}\rangle_1/i\Omega]\int_0^\infty G_0(x, p_1)\,dx \times\left[1 - \frac{1}{[1+i\Omega x]}\right] = [\langle x^{-1}\rangle_1/i\Omega][1 - I_0(\Omega, p_1)], \tag{A.5}$$

where the τ_0 associated with $\Omega \equiv \omega\tau_0$ is that belonging to $I_1(\Omega, p_1)$. Eq. (A.5) shows that one need only calculate $I_0(\Omega, p_1)$ in order to obtain $I_1(\Omega, p_1)$ when $\langle x^{-1}\rangle_1$ is known.

So far, so good, but the problem remains of obtaining accurate and useful expressions for specific KWW response, $I_{Kn}(\Omega, \beta_n)$, because no general expression is known for G_{Kn}. It therefore becomes necessary to calculate $I_{Kn}(\Omega, \beta)$ by either numerical integration or series methods [3,9,25,26]. Although the former approach is useful for checking results of the latter one, accurate calculations by numerical integration without knowledge of G_{Kn} can be very slow, particularly for small β. Since CNLS fitting requires the calculation of very many values of $I_{K0}(\Omega, \beta)$ to obtain a converged fit, such integration is inappropriate for this application. But there are problems with the series approach as well. We shall use two series, one for the low-frequency region (LF) and one for the rest of the frequency range (HF). A problem arises because the intermediate, or transition, region between the two series can involve very slowly convergent or even divergent behavior [3,25]. This problem is solved, as discussed below, by the use of the ϵ-algorithm [43], a procedure included in LEVM which usually allows one to obtain useful results from a relatively small number of partial sums of even a divergent series. It will be convenient to calculate I_{K0} results since those for I_{K1} are then easily obtained. Although three different accuracy levels are available in the LEVM routines, all present results were obtained using the highest-accuracy choice.

A.1. Low-frequency series

An interesting way to develop the LF series is to carry out a Maclaurin expansion of Eq. (2) for the KWW0 case. On interchanging integral and differential operators, one immediately obtains a simple series involving the moments $\langle x^m\rangle_{K0}$ associated with $G_{K0}(x)$. Although no general expression for $G_{K0}(x)$ is known, its moments are given in terms of gamma functions as [9]

$$\langle x^m\rangle_{K0} \equiv \Xi_m = \Gamma(m/\beta)/[\beta\Gamma(m)], \tag{A.6}$$

where the Ξ_m notation is introduced for simplicity, and Ξ_m becomes exceedingly large for large m. Now the series may be expressed as

$$I_{K0}(\Omega) = 1 + \sum_{m=1}^{\infty}(-i\Omega)^m\Xi_m, \tag{A.7}$$

which may be readily separated into real and imaginary parts. This series, a form of one given earlier [3], shows faster convergence the larger β and the smaller Ω. For fixed β, it becomes divergent for a sufficiently large value of Ω. For $\beta = 1$ and $\Omega < 1$, $I_{K0}(\Omega) = [1 + i\Omega]^{-1}$, as it should.

A.2. High-frequency series

Here we use a form of a series given by G. Williams and co-workers [3]. Define a quantity g_m analogous to Ξ_m as

$$g_m = \beta\Gamma(m\beta)/\Gamma(m), \tag{A.8}$$

which decreases as m increases. The series may be written as

$$I_{K0}(\Omega) = \sum_{m=1}^{\infty}(-1)^{m-1}\Omega^{-m\beta}g_m \exp(-im\beta\pi/2). \tag{A.9}$$

It is convergent for $\Omega > 0$, but convergence becomes exceedingly slow as β increases and Ω decreases.

A.3. Series summation and treatment of the transition region

During summation of the series for I'_{K0} and that for I''_{K0}, we calculate the absolute value of the ratio of the $(m+1)$th term to the mth partial sum. Convergence is declared if this quantity is less than a number δ given by 10^{-7}, 10^{-5}, or 10^{-3} for three accuracy levels. If not, summation is continued for a total of N terms. The N partial sums, with N odd, are then input to the ϵ-algorithm, and its output, a diagonal Padé convergent [43], is used as the best

estimate for the value of the function from which the series arose. There is an overlap region on the LF side of the HF series and on the HF side of the LF one where the ϵ-algorithm is needed for both series. Because even double-precision arithmetic is insufficient to allow the ϵ-algorithm to continue to yield high accuracy results as the series convergence/divergence becomes more and more intractable, there is a cross-over value of Ω at which the LF and HF ϵ-algorithm results are the same. At this point and for larger Ω, the HF series is used in place of the LF one. The cross-over point, Ω_c, depends on β, and the following expressions have been found satisfactory for it: for $\beta \geq 0.5$, $\Omega_c = 1.5\beta^{5.41}$, and for $\beta < 0.5$, $\Omega_c = 16.53\beta^{8.91}$. Thus $\Omega_c \simeq 0.035$ for $\beta = 0.5$, and $\Omega_c \simeq 0.0047$ for $\beta = 0.4$. For comparison, the LF series becomes divergent at $\Omega \simeq 0.0125$ and at 0.00143, for these two values of β, respectively.

We use different values of N for the LF and HF series and for $\beta > 0.6$ and $\beta \leq 0.6$. For the three values of δ given above, the values for the LF series are 11, 7, and 5 and 21, 13, and 9, respectively. Similarly for the HF series, the values are 21, 13, and 9, and 43, 27, and 19. For $\beta = 0.5$, the present approximate KWW0 method may be used to fit data calculated with a relative error of 10^{-9} using Eq. (2) with $G_n(x) = G_{K0}(x)$. For 121 points with $10^{-6} \leq \Omega \leq 10^6$, the proportional-weighing S_F values for the three accuracy levels were about 1.1×10^{-7}, 2.4×10^{-6}, and 2.5×10^{-5}, respectively. For other values of β, the tables of Dishon et al. [25] may be used for comparison, although they extend only over the range $10^{-3} \leq \Omega \leq 2500$. For $\beta \neq 0.5$, it is found that even for the highest accuracy choice, the accuracy of the present approximation decreases slightly as β decreases below 0.5, with errors at the cross-over point of the order of 10^{-5} or even 10^{-4} in the close neighborhood of crossover for $\beta \leq 0.2$ or so. The present approach is nevertheless more than adequate for rapid and accurate fitting of experimental data for the range $0.05 \leq \beta < 1$.

References

[1] R. Kohlrausch, Prog. Ann. Phys. Chem. 91 (1854) 179.
[2] G. Williams and D.C. Watts, Trans. Faraday Soc. 66 (1970) 80.
[3] G. Williams, D.C. Watts, S.B. Dev and A.M. North, Trans. Faraday Soc. 67 (1971) 1323.
[4] J.R. Macdonald, J. Appl. Phys. 62 (1987) R51.
[5] J.R. Macdonald and C.A. Barlow Jr., Rev. Mod. Phys. 35 (1963) 940.
[6] J.R. Macdonald and W.J. Thompson, Commun. Stat. Simul. Comput. 20 (1991) 843.
[7] W.J. Thompson and J.R. Macdonald, Am. J. Phys. 59 (1991) 854.
[8] C.T. Moynihan, L.P. Boesch and N.L. Laberge, Phys. Chem. Glasses 14 (1973) 122.
[9] C.P. Lindsey and G.D. Patterson, J. Chem. Phys. 73 (1980) 3348.
[10] J.R. Macdonald, J. Non-Cryst. Solids 197 (1996) 83; erratum J. Non-Cryst. Solids 204 (1996) 309.
[11] A.S. Nowick and B.S. Lim, J. Non-Cryst. Solids 172–174 (1994) 1389.
[12] J.R. Macdonald, Appl. Phys. A59 (1994) 181.
[13] J.R. Macdonald, in: Electrically Based Microstructural Characterization, Proceedings, Fall meeting, November 1995, Boston, MA, Vol. 411 (Materials Research Society, Pittsburgh, PA, 1996) p. 71.
[14] J.R. Macdonald, J. Non-Cryst. Solids, accepted.
[15] K.S. Cole and R.H. Cole, J. Chem. Phys. 9 (1941) 341.
[16] D.W. Davidson and R.H. Cole, J. Chem. Phys. 19 (1951) 1484.
[17] J.R. Macdonald and R.L. Hurt, J. Chem. Phys. 84 (1986) 496.
[18] J.R. Macdonald, J. Appl. Phys. 75 (1994) 1059.
[19] P.B. Macedo, C.T. Moynihan and R. Bose, Phys. Chem. Glasses 13 (1972) 171.
[20] J.R. Macdonald, J. Appl. Phys. 58 (1985) 1955.
[21] H.K. Patel and S.W. Martin, Phys. Rev. B45 (1992) 10292.
[22] C.T. Moynihan, J. Non-Cryst. Solids 172–174 (1994) 1395.
[23] H. Jain and C.H. Hsieh, J. Non-Cryst. Solids 172–174 (1994) 1408.
[24] K.L. Ngai and A.K. Rizos, Phys. Rev. Lett. 76 (1996) 1296.
[25] M. Dishon, G.H. Weiss and J.T. Bendler, J. Res. Natl. Bur. Stand. 90 (1985) 27.
[26] G.H. Weiss, J.T. Bendler and M. Dishon, J. Chem. Phys. 83 (1985) 1424.
[27] J.R. Macdonald, J. Chem. Phys. 102 (1995) 6241.
[28] S.R. Elliott, J. Non-Cryst. Solids 170 (1994) 97.
[29] J.C. Dyre, J. Non-Cryst. Solids 135 (1991) 219.
[30] J.R. Macdonald and L.D. Potter Jr., Solid State Ionics 23 (1987) 61.
[31] Private communication.
[32] H. Schütt and E. Gerdes, J. Non-Cryst. Solids 144 (1992) 1, 14.
[33] J.R. Macdonald, ed., Impedance Spectroscopy — Emphasizing Solid Materials and Systems (Wiley-Interscience, New York, 1987).
[34] J.R. Macdonald, Solid State Ionics 25 (1987) 271.
[35] S.R. Elliott, J. Non-Cryst. Solids 170 (1994) 97.
[36] J.R. Macdonald, Solid State Ionics 15 (1985) 159.
[37] R.L. Hurt and J.R. Macdonald, Solid State Ionics 20 (1986) 111.

[38] A.S. Nowick, B.S. Lim and A.V. Vaysleyb, J. Non-Cryst. Solids 172–174 (1994) 1243.
[39] H.P. Schwan, in: Advances in Biological and Medical Physics, eds. J.H. Lawrence and C.A. Tobias (Academic Press, New York, 1957) pp. 147–209, see pp. 160–161.
[40] D. Ravaine and J.-L. Souquet, C. R. Acad. Sci. (Paris) 277C (1973) 489.
[41] S. Havriliak and S. Negami, J. Polym. Sci. C14 (1966) 99.
[42] C.T. Moynihan, J. Non-Cryst. Solids 203 (1996) 359.
[43] J.R. Macdonald, J. Appl. Phys. 35 (1964) 3034.